Modeling and Calculation of the LiF−NaF−MF_3 (M = La, Ce, Pu) Phase Diagrams

J. P. M. van der Meer,*,† R. J. M. Konings,† K. Hack,‡ and H. A. J. Oonk§

European Commission, Joint Research Centre, Institute for Transuranium Elements, P.O. Box 2340, 76125 Karlsruhe, Germany, GTT-Technologies, Kaiserstrasse 100, 52134 Herzogenrath, Germany, and Petrology Group, Faculty of Geosciences, Utrecht University, Budapestlaan 4, 3584 CD Utrecht, The Netherlands

Received July 14, 2005. Revised Manuscript Received November 8, 2005

The ternary systems LiF−NaF−LaF_3 and LiF−NaF−CeF_3 have been experimentally analyzed and thermodynamically assessed. Two models were used and compared to describe the excess Gibbs terms of the binary subsystems. One was a regular polynomial description of the excess terms, the other a quasichemical in the quadruplet approximation. In both cases, a fine agreement with the experimental data was achieved, after asymmetrical extrapolation from the binary to the ternary systems. The binary systems of the related actinide system LiF−NaF−PuF_3 were assessed, making use of experimental data known from the literature. The lanthanide systems served as a proxy for LiF−NaF−PuF_3 to calculate the ternary phase diagram.

1. Introduction

The Molten Salt Reactor (MSR) is one of the nuclear systems of Generation IV. A first prototype MSR was built in the 1960s in the United States, at Oak Ridge National Laboratory, during the Molten Salt Reactor Experiment. Many thermodynamic studies related to the fuel compositions foreseen were performed in that period.[1−4] But interest ceased in the 1970s, and financial flows shifted to other nuclear projects. Nowadays, the MSR is a subject of renewed interest, as it is a safe and efficient system with a potentially high fuel burnup and the possibility for actinide burning.

The fuel for a MSR consists of a fissile material, such as ^{233}U, ^{235}U, ^{239}Pu, or other higher actinides, dissolved as a fluoride salt in a matrix of several metal fluorides that have the appropriate chemical and neutronic properties. When designed as an actinide burner, a potential solvent is a eutectic melt of LiF and NaF, because higher solubilities can be reached for PuF_3 and other actinide trifluorides than in a traditional LiF−BeF_2 solvent.[5]

Experimental data are available for the binary subsystems, but to the best of our knowledge, data on the ternary phase diagram have not been published so far. This scarcity of data is not an exception, and when no experimental data are available, the only way to predict phase behavior of multicomponent systems is thermodynamic modeling of the binary systems of interest, which can be extended to higher-order systems. This was all done according to the CALPHAD method. It includes the critical review of all available data on the systems of interest, followed by an interactive assessment so that the best agreement is obtained between experimental data and thermodynamic parameters. In the thermodynamist community, it has been widely accepted as the most sophisticated way to treat practical problems, such as the applicability of molten salts for nuclear purposes, with the aid of fundamental thermodynamics.

In this study we first performed thermodynamic assessments on binary subsystems of LiF−NaF−LaF_3 and LiF−NaF−CeF_3. Excess Gibbs energy terms were optimized according to a general polynomial description. The system LiF−NaF−LaF_3 was also assessed using the modified quasichemical model in the quadruplet approximation proposed by Pelton and Chartrand.[6,7] For the optimization, our own experimental DSC data and data found in the literature were used. After extrapolation according to the Kohler−Toop model,[8] the ternary diagrams were calculated. The results were compared to our own experimental data for the ternary systems. Using the two lanthanide analogues as a proxy, we present the LiF−NaF−PuF_3 diagram, which was calculated from the known binaries, and in a similar manner.

2. Experimental Section

The thermal analysis on the salt samples was performed with differential scanning calorimetry, using a Netzsch STA 449C Jupiter. Because fluoride salts are hygroscopic, sample preparation and measurements were carried out in an inert argon atmosphere. LiF (99.98%), NaF (99.99%; on a metals basis), and LaF_3 (99.99%;

* To whom correspondence should be addressed. E-mail: Juliette.VAN-DER-MEER@cec.eu.int.
† Institute for Transuranium Elements.
‡ GTT-Technologies.
§ Utrecht University.

(1) Grimes, W. R.; Cuneo, D. R. *Reactor Handbook*; Interscience Publishers, Inc.: New York, 1960; Vol. I: Materials, Chapter 17, p 425.
(2) Grimes, W. R. *Nucl. Appl. Technol.* **1969**, *8*, 137.
(3) Baes, C. F., Jr. *J. Nucl. Mater.* **1974**, *51*, 149.
(4) MacPherson, H. G. *Nucl. Sci. Eng.* **1985**, *90*, 374.
(5) Mailen, J. C.; Smith, F. J.; Ferris, L. M. *J. Chem. Eng. Data* **1971**, *16*, 68.
(6) Pelton, A. D.; Chartrand, P.; Eriksson, G. *Metall. Trans. A* **2001**, *32*, 1409.
(7) Chartrand, P.; Pelton, A. D. *Metall. Trans. A* **2001**, *32*, 1417.
(8) Pelton, A. D. *CALPHAD* **2001**, *25*, 319.

10.1021/cm051531v CCC: $33.50
Published on Web 12/15/2005

Table 1. ΔH^0_f(298.15) (kJ mol^{-1}), S^0(298.15) (J K^{-1} mol^{-1}), and C_p Data for the Pure Components and Intermediate Compounds of the LiF−NaF−MF$_3$ System, with M = La, Ce, Pu

compd	$\Delta_f H^0$(298.15)	S^0(298.15)	a_0	a_1T	c_2T^2	$a_{-2}T^{-2}$
LiF(l)[a]	−598.654	42.962	64.183			
NaF(l)[a]	−558.583	50.778	72.989			
LaF_3(l)[a]	−1633.920	97.639	135.00			
CeF_3(l)[a]	−1650.932	116.739	130.61			
PuF_3(l)[a]	−1568.813	109.331	130.00			
LiF(cr)[a]	−616.931	35.660	43.309	1.6312×10^{-2}	5.0470×10^{-7}	-5.6912×10^{5}
NaF(cr)[a]	−576.650	51.210	42.554	1.9881×10^{-2}		-3.8773×10^{5}
LaF_3(cr)[a,b]	−1669.500	106.980	122.119	-2.2467×10^{-2}	-1.6309×10^{-5}	-2.1714×10^{6}
CeF_3(cr)[a]	−1689.200	118.700	103.258	-1.2990×10^{-2}	2.4688×10^{-5}	-7.2087×10^{5}
PuF_3(cr)[a]	−1586.694	126.110	104.078	7.07×10^{-4}		-1.0355×10^{6}
NaF·LaF_3(cr)[c]	−2254.924	155.515	165.00	-5.4388×10^{-3}	-1.6309×10^{-5}	-2.2682×10^{6}
NaF·CeF_3(cr)[c]	−2308.680	135.160	145.812	6.8911×10^{-3}	2.469×10^{-5}	-1.1086×10^{6}
NaF·PuF_3(cr)[c]	−2221.946	130.110	146.910	1.7736×10^{-2}		-1.1323×10^{6}

[a] Data taken from an internal report.[31] [b] An extra term in the C_p function: $2.8175 \times 10^6 T$.[3] [c] Obtained by assessment with the polynomial model.

REO), all from Alfa Aesar, were used. Before use, the salts were dried in a furnace for 5 h at 523 K under a continuous Ar 6.0 flow. Weighted mixtures were put in boron nitride crucibles. After being closed with a screwed cap, the crucibles were transported immediately to the DSC apparatus, where the measurements were performed.

All the samples underwent two heating cycles. The first had to be discarded, because it was assumed that mixing was not yet complete. Only the heating curves from the second cycle were analyzed. Onset temperatures were taken for the determination of eutectic and peritectic temperatures. However, for the determination of the liquidus, the endset temperature[9] was selected. This was done for the following reason. In contrast to an isothermal effect, which gives a clearly defined signal, a liquidus peak has a different character. When we increase the temperature for a certain composition, the amount of liquid phase present increases gradually, until the moment when the last solid crystal disappears. That moment is usually marked by a little cusp in the DSC spectrum. Moreover, taking the endset point as the temperature at which the melting process is complete is also in accordance with the definition of a liquidus. This assumes that the liquidus temperature is the lowest temperature at a specified composition, above which only the liquid phase is present.

Table 3 lists the results of the DSC experiments on binary mixtures of LiF−LaF_3, LiF−CeF_3, NaF−LaF_3, and NaF−CeF_3.

3. Thermodynamic Assessment

3.1. Optimization of Gibbs Energy Coefficients. Gibbs energy functions of all phases of the system, including the excess Gibbs energy coefficients of the respective phases if that is a solution, are necessary for describing a T−X phase diagram. When the functions are unknown, which is in general the case for the excess Gibbs terms, they can be obtained by performing a thermodynamic assessment. The missing coefficients in the Gibbs energy as well as in the excess equations are optimized so that a best fit is found between the known Gibbs energy functions of the compounds and the available experimental data.

The Gibbs energy functions for the relevant compounds are usually set up after careful investigation of thermodynamic tables.[10] The function is described by eq 1 as the contribution of the enthalpy of formation and the absolute entropy at the reference state plus a contribution of the heat capacity C_p as a polynomial function of T.

$$G(T) = \Delta_f H^0(298.15) + S^0(298.15)T + \sum a_i T^i \qquad (1)$$

For the pure compounds LiF, NaF, LaF_3, CeF_3, and PuF_3, thermodynamic data were taken from the literature. This was not the case for the intermediate compounds NaF−MF_3 (M = La, Ce, Pu). Their Gibbs energy equations were obtained by optimization. The equations for the pure compounds were added in weighted average. It was assumed that, according to the Neumann−Kopp rule, C_p could be added in weighted average, whereas the enthalpy and entropy of formation needed to be assessed. Table 1 lists these parameters for the literature data as well as the assessed values.

General polynomials were used to describe the excess Gibbs energy coefficients that define the shape of a phase diagram. The equation for a binary system A−B is given in eq 2.

$$\Delta G_{xs} = \sum_{p,q}^{n} L^{p,q}_{A,B}(T) Y_A \left(\frac{\chi_i}{\chi_i + \chi_j}\right)^p Y_B \left(\frac{\chi_j}{\chi_i + \chi_j}\right)^q \qquad (2)$$

$L^{p,q}_{A,B}(T)$ is the excess Gibbs energy term as a function of the temperature. Y_A and Y_B are the equivalent fractions of the components, whereas χ_i and χ_j are the sum of the equivalent fractions in the same symmetry group with i and j as indices for the group numbers. It should be noted that it is possible to rewrite the well-known Redlich−Kister equation for binary interactions in the general polynomial notation in this case, as the equivalent fractions are similar to the mole fractions.

For the quasichemical quadruplet approximation, first-nearest and second-nearest neighbor short-range ordering in the liquid phase are considered at the same time.[6] It is assumed that the solution consists of two sublattices. This implies, for an AX−BY molten salt, that the cations (A and B) are allocated to sublattice I, whereas the anions X and Y belong to sublattice II. The following exchange reaction is considered

$$A{-}X + B{-}Y \rightleftharpoons A{-}Y + B{-}X \quad \Delta g^{exchange}_{AB/XY} \qquad (3)$$

It should be noted that each quadruplet consists of two cations and two anions, where the cation−anion pair

(9) Höhne, G. W. H.; Cammenga, H. K.; Eysel, W.; Gmelin, E.; Hemminger, W. *Thermochim. Acta* **1990**, *160*, 1.
(10) Chase, M. W., Jr., Ed. *NIST-JANAF Thermochemical Tables*, 4th ed.; Journal of Physical and Chemical Reference Data Monograph 9; AIP Press/Springer-Verlag: New York, 1998.

Table 2. Optimized Excess Gibbs Parameters of the Liquid Phase for LiF−NaF, LiF−MF_3, and NaF−MF_3, by the Polynomial Model

A−B	*p*	*q*	${}^0L_{A,B}$ (J mol^{-1})	${}^1L_{A,B}$ (J K^{-1} mol^{-1})
NaF−LiF	0	0	−5468.2	1.5505
	0	1	5133.2	−6.9989
LaF_3−LiF	0	0	−30371	17.023
CeF_3−LiF	0	0	−33179	19.980
PuF_3−LiF	0	0	3809.5	−9.0628
NaF−LaF_3	0	0	−67708	128.27
	1	0	−10990	14.895
	0	1	9563.4	−13.882
CeF_3−NaF	0	0	−34066	9.2741
	0	1	−26229	−0.187
PuF_3−NaF	0	0	−45790	74.016
	1	0	15172	−63.492
	0	1	−49495	−10.000

produces a first-nearest neighbor (FNN) interaction and the cation−cation and anion−anion pairs exert second-nearest neighbor (SNN) interactions. Because the only anion involved in this study is F^-, the quadruplet approximation is, in principle, reduced to the so-called pair approximation with two sublattices.[11] However, the quadruplet notation is kept here. The excess Gibbs energy can be expressed as SNN interaction terms $\Delta g_{AB/X_2}$, and can be expanded as a polynomial

$$\Delta g_{AB/X_2} = \Delta g^0{}_{AB/X_2} + \sum_{(i+j)\geq 1} \chi^i_{AB/X_2} \chi^j_{BA/X_2} g^{ij}_{AB/X} \qquad (4)$$

where χ^i_{AB/X_2} and χ^j_{BA/X_2} are the mole fraction ratios of the summation of symmetric and asymmetric cation−cation and anion−anion pairs, respectively.

FactSage 5.3[12] was used to obtain optimized values for the interaction coefficients in the polynomial approach, for the quadruplet approach as well as for unknown parameters in the Gibbs energy equations of intermediate compounds, in a way that they was in best agreement with both the known theoretical Gibbs energy equations and the experimental data. The OptiSage module from FactSage uses the Bayesian optimization algorithm.[13] Its concept is based on the estimation of a probability distribution function, given an experimental data set and prior solutions, to generate new candidate solutions.

The optimized excess Gibbs terms for the quasichemical model with quadruplets are listed below (see Table 2). The same notation as that proposed by Chartrand and Pelton[7,14,15] is used here. For a La^{3+}−F^-−Na^+−F^- quadruplet, the excess Gibbs terms were found to be

$$\Delta g_{LaNa/FF} = 908.25 - 14.974T - 9168.3\chi_{LaNa} + 2936.7\chi_{NaLa} \text{ J mol}^{-1} \qquad (5)$$

Similar equations were found for the other quadruplets.

$$\Delta g_{LaLi/FF} = -192.06 - 5.0976T + 718.44\chi_{LaLi} + 2138.1\chi_{LiLa} \text{ J mol}^{-1} \qquad (6)$$

$$\Delta g_{NaLi/FF} = 662.68 - 2.8405T + 1374.7\chi_{NaLi} + 487.40\chi_{LiNa} \text{ J mol}^{-1} \qquad (7)$$

3.2. Calculations for Ternary Systems. By extrapolation of the acquired excess coefficients of the three binary subsystems LiF−NaF, LiF−MF_3, and NaF−MF_3, where M = La, Ce, Pu, we obtained the ternary system LiF−NaF-MF_3. To start, it was assumed there were no ternary interactions. The extrapolation of the excess terms was done in an asymmetrical way according to the Kohler−Toop method, as the ternary system is asymmetric, i.e., one component is chemically different from the other two. In the LiF−NaF−MF_3 systems, the trifluoride was selected as the asymmetric component in the extrapolation. This asymmetrical treatment of the ternary system was carried out for both the polynomial and quasichemical models.

In the quasichemical model, we chose to introduce small ternary terms as in eq 4. They were included when the binary systems were expanded to a ternary. The ternary interaction terms arising from the interaction between system A−B and some C are described in eq 8.

$$\Delta g_{AB(C)/X_2} = \sum_{i\geq 0, j\geq 0, k\geq 1} \chi^i_{AB/X_2} \chi^j_{BA/X_2} \left(\sum g^{ijk}_{AB(C)/X_2} \frac{X_{C/X}}{Y_X} (1 - \xi_{AB/X_2} - \xi_{BA/X_2})^{k-1} \right) \qquad (8)$$

$X_{C/X}$ is a pair fraction, Y_X, as previously stated, is the coordination equivalent fraction of component X, and ξ_{AB/X_2} and ξ_{BA/X_2} are defined as the sums of $X_{A/X}/Y_X$ and $X_{B/X}/Y_X$.[6,16]

Small ternary interactions terms in the quadruplet La^{3+}−F^-−Na^+−F^- due to the interaction with Li were found to be

$$g^{001}_{LaNa(Li)/F} = 536.98 \text{ J mol}^{-1} \qquad (9)$$

and

$$g^{011}_{LaNa(Li)/F} = -348.30 \text{ J mol}^{-1} \qquad (10)$$

Idem were the ternary interactions terms in La^{3+}−F^-−Li^+−F^- with Na

$$g^{001}_{LaLi(Na)/F} = 69.160 \text{ J mol}^{-1} \qquad (11)$$

and

$$g^{011}_{LaLi(Na)/F} = 26.512 \text{ J mol}^{-1} \qquad (12)$$

and in Na^{3+}−F^-−Li^+−F^- with La

$$g^{001}_{NaLi(La)/F} = 436.23 \text{ J mol}^{-1} \qquad (13)$$

and

$$g^{011}_{NaLi(La)/F} = 826.85 \text{ J mol}^{-1} \qquad (14)$$

4. Results and Discussion

4.1. The Binary Subsystems. The phase diagrams of LiF−NaF and LiF−MF_3 are single eutetic systems.

(11) Chartrand, P.; Pelton, A. D. *Metall. Trans. A* **2001**, *32*, 1397.
(12) Bale, C. W.; Chartrand, P.; Degterov, S. A.; Eriksson, G.; Hack, K.; BenMahfoud, R.; Melançon, J.; Pelton, A. D.; Petersen, S. *CALPHAD* **2002**, *62*, 189.
(13) Pelikan, M.; Goldberg, D. E.; Cantú-Paz, E. In *Proceedings of the Genetic and Evolutionary Computation Conference*; Meeting of the International Society for Genetic and Evolutionary Computation, Orlando, FL, 1999; p 525.
(14) Chartrand, P.; Pelton, A. D. *Metall. Trans. A* **2001**, *32*, 1361.
(15) Chartrand, P.; Pelton, A. D. *Metall. Trans. A* **2001**, *32*, 1385.
(16) Pelton, A. D.; Chartrand, P. *Metall. Trans. A* **2001**, *32*, 1355.

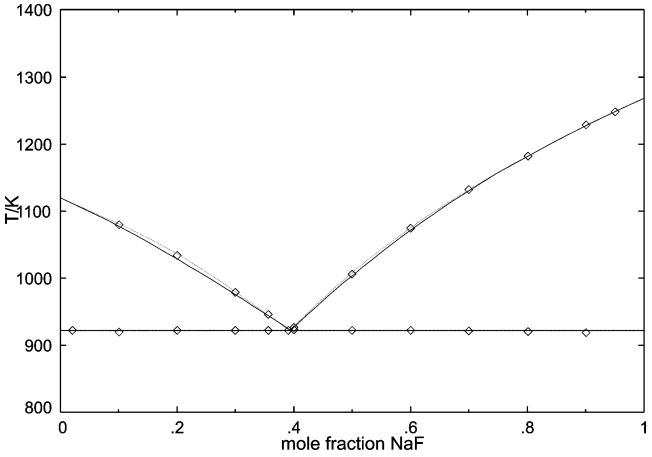

Figure 1. Calculated diagrams of LiF−NaF. Solid line, polynomial model; dashed line, quasichemical model. Data are from Holm and Kleppa.[29]

NaF−MF$_3$, on the other hand, contains an intermediate compound, NaF·MF$_3$, which melts incongruently.

Different sets of experimental data exist for LiF−LaF$_3$[17−20] and NaF−LaF$_3$,[20,21] and they have the largest variations at the LaF$_3$-rich side of the diagram. This is probably the case for the CeF$_3$ and PuF$_3$ analogues as well, but fewer data[22−24] are available to make a proper comparison. During the optimization, it is important to distinguish between the different experimental sets, and to select the one that seems most correct. When all the sets are taken into account, unwanted curves may appear in the calculated diagram.

It appeared that the optimized excess parameters, which were obtained by including only literature data, gave an unsatisfactory result after extrapolation to the ternary system, especially for the liquidus at LaF$_3$-rich compositions. Therefore, a number of experiments on binary mixtures at the LaF$_3$ side were redone in this study as well, and the results were included in the assessment. More weight was given to our own experimental data to carry out the optimization of the excess parameters. This resulted consequently in a better fit with the ternary experimental data afterward, as the experiments were performed under the same conditions and the peak analysis was done in a similar way, which cannot be said for those data reported in the literature.

The excess parameters of the binary systems LiF−NaF, LiF−LaF$_3$, and NaF−LaF$_3$ were optimized using both the polynomial and quadruplet models. In Figures 1, 2, and 5, the two phase diagrams obtained by the different models are shown together. It can be seen that the differences are minor. Figures 3 and 4 show the phase diagrams for LiF−CeF3 and LiF−PuF3, respectively, and Figures 6 and 7 show the diagrams for NaF−CeF$_3$ and NaF−PuF$_3$, respectively.

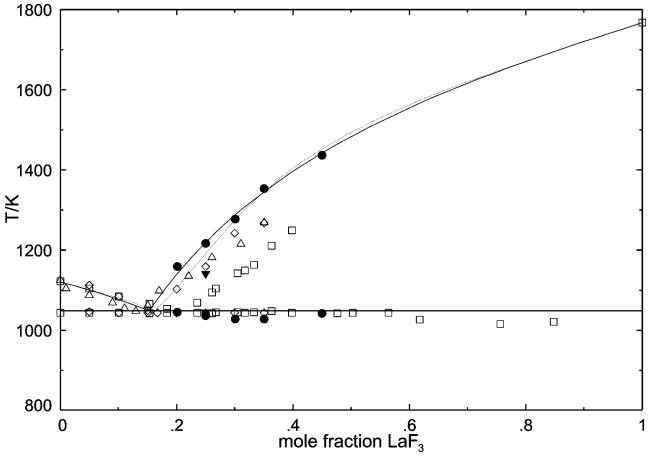

Figure 2. Calculated diagrams of LiF−LaF$_3$. Solid line, polynomial model; dashed line, quasichemical model. Closed circles, experimental data; open triangles, Bukhalova and Babaeva;[18] open squares, Khripin;[17] closed reversed triangles, Thoma et al.;[19] open diamonds, Agulyanskii and Bessonova.[20] These data were erroneously assigned to Thoma et al. in a previous paper.[30]

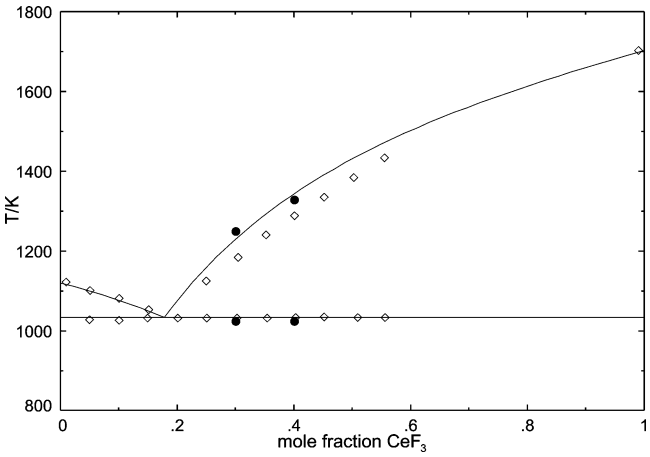

Figure 3. Calculated diagram of LiF−CeF$_3$. Closed circles, experimental data; open diamonds, Barton et al.[22]

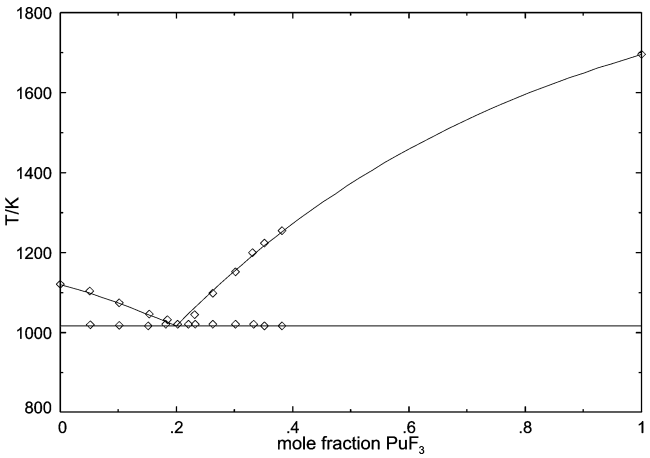

Figure 4. Calculated diagram of LiF−PuF$_3$. Data from Barton et al.[23]

Table 4 lists all the calculated invariant equilibria in the above-mentioned binary systems, giving the results for the polynomial model as well as for the quasichemical model.

It can be seen in Figures 2 and 3 that the largest differences between the new experimental data and those from the

(17) Khripin, L. A. *Izv. Sib. Otd. Akad. Nauk SSSR, Ser. Khim. Nauk* **1963**, *7*, 107.
(18) Bukhalova, G. A.; Babaeva, E. P. *Russ. J. Inorg. Chem.* **1965**, *10*, 1026.
(19) Thoma, R. E.; Brunton, G. D.; Penneman, R. A.; Keenan, T. K. *Inorg. Chem.* **1970**, *9*, 1096.
(20) Agulyanskii, A. I.; Bessonova, V. *Russ. J. Inorg. Chem.* **1982**, *27*, 579.
(21) Abdoun, F.; Gaune-Escard, M.; Hatem, G. *J. Phase Equilib.* **1997**, *18*, 6 and references therein.
(22) Barton, C. J.; Bratcher, L. M.; Sheil, R. J.; Grimes, W. R. Oak Ridge National Laboratory, Oak Ridge, TN. Unpublished work, 2005.
(23) Barton, C. J.; Strehlow, R. A. *J. Inorg. Nucl. Chem.* **1961**, *18*, 143.
(24) Barton, C. J.; Redman, J. D.; Strehlow, R. A. *J. Inorg. Nucl. Chem.* **1961**, *20*, 45.

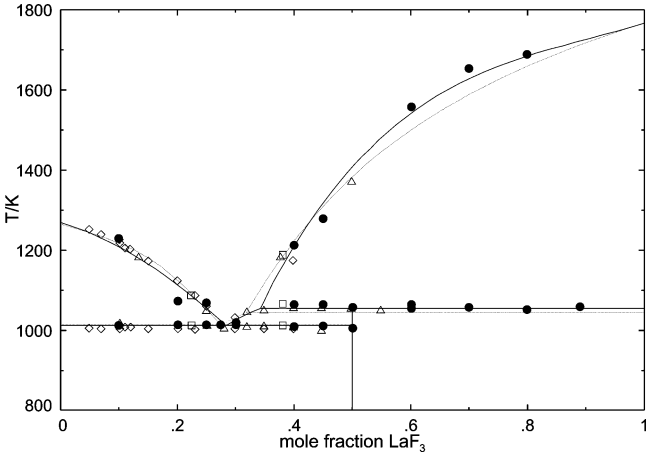

Figure 5. Calculated diagrams of $NaF-LaF_3$. Solid line, polynomial model; dashed line, quasichemical model. Closed circles, experimental data; open triangles, Abdoun et al.;[21] open diamonds, Matthes and Holz (1962); open squares, Grande (1992). The last two are references in ref 21.

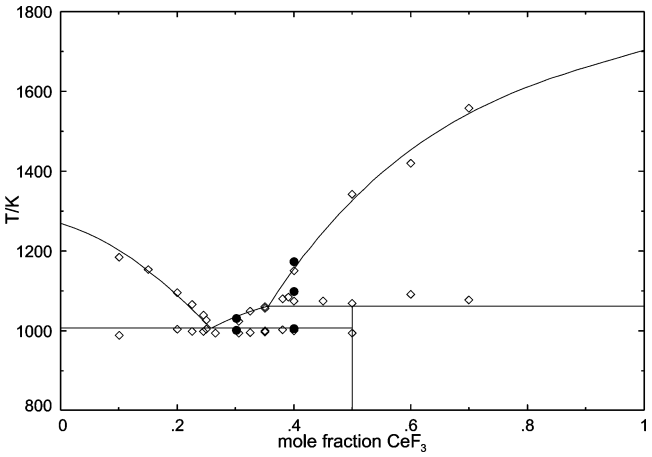

Figure 6. Calculated diagram of $NaF-CeF_3$. Closed circles, experimental data; open diamonds, Barton et al.[24]

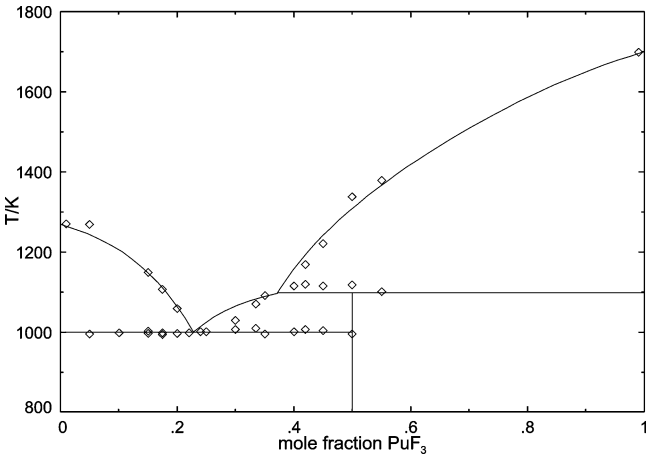

Figure 7. Calculated diagram of $NaF-PuF_3$. Data from Barton et al.[24]

literature arise in the LaF_3, c.q. CeF_3 side. This is probably caused by the difficulty in obtaining a clear DSC signal at the liquidus temperature, considering the reasons given in the Experimental Section. However, the different series of data are consistent on their own. Care was taken to obtain a satisfying diagram, preferably in agreement with the present data, as the shapes of the binary diagrams greatly influence the ternary diagram.

Table 3. DSC Data, Interpreted as Eutectic, Peritectic, and Liquidus Temperature, in $LiF-MF_3$ and $NaF-MF_3$, with M = La, Ce

mole fraction	T_{eut} (K)	T_{per} (K)	T_{liq} (K)
0.201 LaF_3/(LiF+LaF_3)	1043.9		1158.0
0.250 LaF_3/(LiF+LaF_3)	1035.5		1215.7
0.301 LaF_3/(LiF+LaF_3)	1027.0		1277.1
0.350 LaF_3/(LiF+LaF_3)	1027.6		1353.3
0.450 LaF_3/(LiF+LaF_3)	1040.9		1435.8
0.301 CeF_3/(LiF+CeF_3)	1022.7		1248.0
0.401 CeF_3/(LiF+CeF_3)	1022.3		1328.0
0.100 LaF_3/(NaF+LaF_3)	1013.6		1228.3
0.201 LaF_3/(NaF+LaF_3)	1014.8		1072.7
0.250 LaF_3/(NaF+LaF_3)	1014.6		1067.6
0.275 LaF_3/(NaF+LaF_3)	1015.5		
0.301 LaF_3/(NaF+LaF_3)	1014.8		1018.8
0.400 LaF_3/(NaF+LaF_3)	1010.2	1064.4	1212.1
0.449 LaF_3/(NaF+LaF_3)	1012.3	1064.2	1278.2
0.500 LaF_3/(NaF+LaF_3)	1005.6	1056.6	
0.601 LaF_3/(NaF+LaF_3)		1054.0	
0.601 LaF_3/(NaF+LaF_3)		1063.9	1558.1
0.700 LaF_3/(NaF+LaF_3)		1056.8	
0.700 LaF_3/(NaF+LaF_3)		1057.0	1652.8
0.799 LaF_3/(NaF+LaF_3)		1051.4	1688.8
0.890 LaF_3/(NaF+LaF_3)		1058.3	
0.301 CeF_3/(NaF+CeF_3)	1000.7		1052.1
0.400 CeF_3/(NaF+CeF_3)	1004.8	1098.4	1248.1

Table 4. Equilibria in LiF−NaF, LiF−MF_3, and NaF−MF_3 According to the Polynomial Model[a]

equilibrium	T (K)	mole fraction
eutectic	921.9	0.394 NaF/(LiF+NaF)
eutectic	*921.4*	*0.392 NaF/(LiF+NaF)*
eutectic	1046.3	0.154 LaF_3/(LiF+LaF_3)
eutectic	*1046.9*	*0.161 LaF_3/(LiF+LaF_3)*
eutectic	1030.8	0.178 CeF_3/(LiF+CeF_3)
eutectic	1016.2	0.200 PuF_3/(LiF+PuF_3)
eutectic	1011.5	0.283 LaF_3/(NaF+LaF_3)
eutectic	*1011.5*	*0.274 LaF_3/(NaF+LaF_3)*
peritectic	1054.6	0.342 LaF_3/(NaF+LaF_3)
peritectic	*1046.2*	*0.318 LaF_3/(NaF+LaF_3)*
eutectic	1004.7	0.257 CeF_3/(NaF+CeF_3)
peritectic	1062.3	0.357 CeF_3/(NaF+CeF_3)
eutectic	1000.0	0.227 PuF_3/(NaF+PuF_3)
peritectic	1097.7	0.373 PuF_3/(NaF+PuF_3)

[a] Values in italics are those found for the quasichemical model in quadruplet approximation.

Differences in the diagrams obtained by the different models exist as well, but they are relatively small. The largest difference is in the $NaF-LaF_3$ system, in the way the two models for the liquid interplay with the enthalpy and entropy of formation of the intermediate compound, which is expressed as a difference in the peritectic point. Nevertheless, both diagrams appear to be reasonable fits of the available data. As can be found in Table 1, the optimized values of the enthalpy of formation and entropy of the $NaF{\cdot}LaF_3$ compound at $T = 298.15$ K result in an enthalpy of formation value of -8.774 kJ mol^{-1} and an entropy of formation value of 2.675 J K^{-1} mol^{-1} from the pure components NaF and LaF_3. Although these values result from purely numerical means, it seems the values are realistic. They were therefore also used in the quasichemical model, where they provided a better result than that of a renewed optimization, which has been tested. However, the authors realize that improvements can possibly be achieved by executing calorimetric experiments on the formation of this compound.

4.2. The Ternary LiF−NaF−MF_3 Phase Diagrams. The calculated ternary diagrams of the systems $LiF-NaF-LaF_3$, $LiF-NaF-CeF_3$, and $LiF-NaF-PuF_3$, obtained after ex-

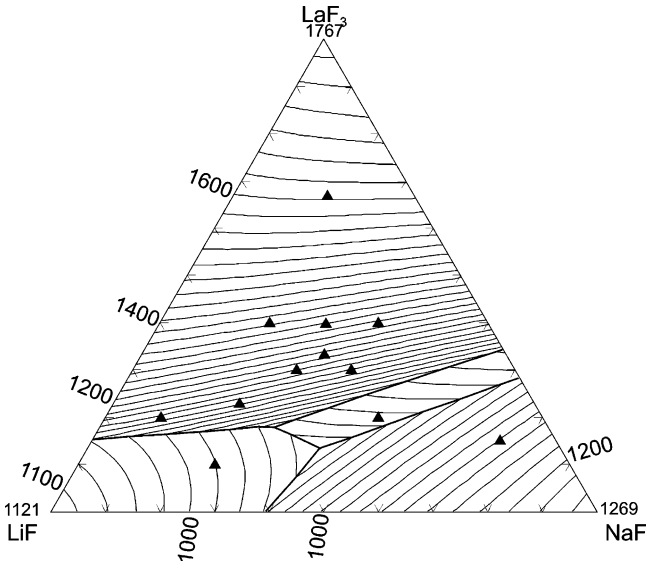

Figure 8. Calculated liquid surface of LiF−NaF−LaF$_3$ by the polynomial model. Isotherms are labeled in K, with an interval of 25 K. Experimental data points are shown as well, of which the liquidus temperatures can be found in Table 6.

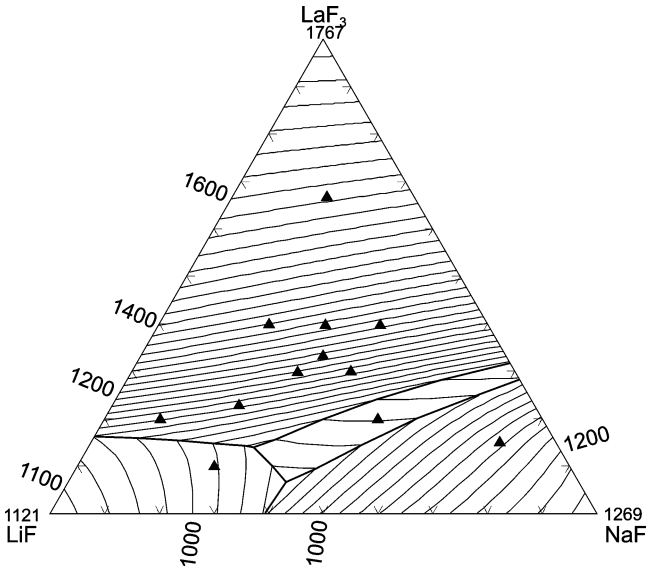

Figure 9. Calculated liquid surface of LiF−NaF−LaF$_3$ by the quasichemical model. Isotherms are labeled in K, with an interval of 25 K. The liquidus temperatures of the experimental data points can be found in Table 6.

trapolation of the excess Gibbs energy terms of the binaries according to the polynomial model, are shown in Figures 8, 10, and 11, respectively. Figure 9 shows the LiF−NaF−LaF$_3$ diagram obtained by the quasichemical model. Table 5 lists all the ternary invariant equilibrium points.

As can be seen, the shapes of the diagrams are similar, which could be expected on the basis of the binary diagrams. They all have a ternary eutectic point close to the LiF−NaF axis and a ternary peritectic, which is slightly richer in LiF−MF$_3$ composition.

The experimental values of the ternary systems were compared with the results of the equilibrium calculations. For systems LiF−NaF−LaF$_3$ and LiF−NaF−CeF$_3$, the calculations were done with the polynomial model, and in the case of LiF−NaF−LaF$_3$, for the quadruplet model as well. This was done by determining the precipitation

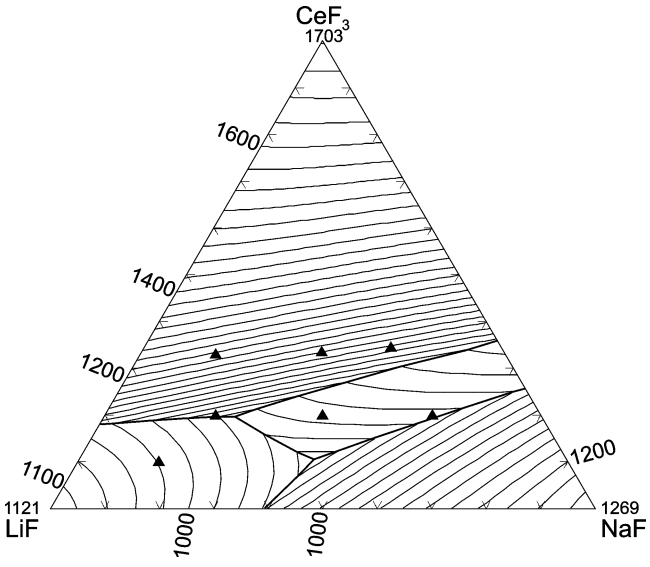

Figure 10. Calculated liquid surface of LiF−NaF−CeF$_3$. Isotherms are labeled in K, with an interval of 25 K. The liquidus temperatures of the experimental data points can be found in Table 6.

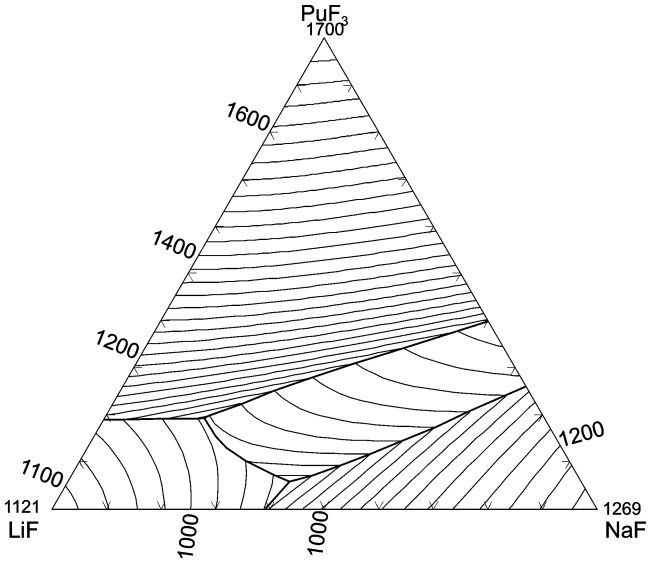

Figure 11. Calculated liquid surface of LiF−NaF−PuF$_3$. Isotherms are labeled in K, with an interval of 25 K.

Table 5. Equilibria in LiF−NaF−MF$_3$[a]

M	equilibrium	*T* (K)	X = LiF	X = NaF	X = MF$_3$
La	eutectic	874	0.441	0.425	0.134
	peritectic	909	0.501	0.321	0.178
La	*eutectic*	*907*	*0.534*	*0.399*	*0.067*
	peritectic	*942*	*0.558*	*0.304*	*0.138*
Ce	eutectic	884	0.465	0.430	0.105
	peritectic	936	0.561	0.243	0.196
Pu	eutectic	906	0.537	0.405	0.058
	peritectic	971	0.625	0.182	0.193

[a] Values in italics are those found for the quasichemical model in quadruplet approximation.

temperature from the liquid phase by using the Equilib module in FactSage 5.3. The ternary data points with the accompanying experimental liquidus temperature and calculated precipitation temperature are listed in Table 6. The difference between the experimental liquidus temperature T_{exp} and the calculated precipitation temperature T_{calc} was normalized by T_{exp}. This deviation is plotted versus T_{exp} in Figure 12 for the systems LiF−NaF−LaF$_3$ and LiF−NaF−CeF$_3$.

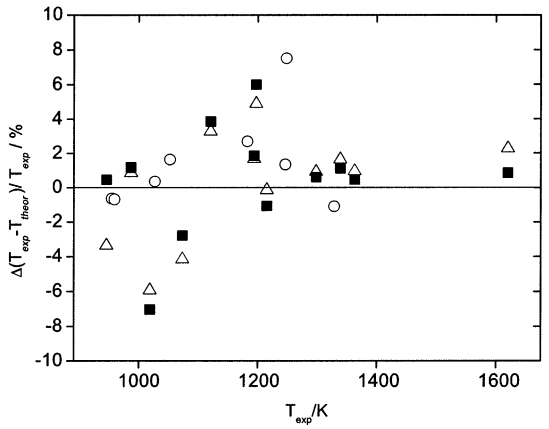

Figure 12. Deviation of the model precipitation temperature from the experimental liquidus temperature, normalized by the experimental temperature, as a percentage vs the experimental temperature. Black squares are for LiF−NaF−LaF_3 in the polynomial model; open triangles are for LiF−NaF−LaF_3 in the quasichemical quadruplet model; open circles are for LiF−NaF−CeF_3.

Table 6. Experimental and Calculated Liquidus Temperatures in LiF−NaF−LaF_3 (polynomial and quasichemical model) and LiF−NaF−CeF_3 (polynomial)

M	X = LiF	X = NaF	X = MF_3	$T_{liq,exp}$	$T_{liq,theor,pol}$	$T_{liq,theor,qua}$
La	0.102	0.748	0.150	1073.1.	1102.8	1117.6
	0.159	0.172	0.669	1620.0	1606.2	1583.0
	0.197	0.404	0.399	1298.2	1290.3	1286.6
	0.298	0.304	0.398	1338.8	1323.8	1317.3
	0.299	0.400	0.301	1197.5	1125.6	1138.5
	0.301	0.499	0.200	945.5	941.1	977.5
	0.333	0.333	0.334	1215.6	1228.5	1218.2
	0.400	0.200	0.400	1363.3	1357.0	1350.6
	0.398	0.303	0.299	1194.1	1171.8	1174.0
	0.540	0.232	0.228	1120.6	1077.3	1083.4
	0.649	0.251	0.100	986.8	975.2	978.3
	0.699	0.102	0.199	1018.5	1090.0	1078.3
Ce	0.199	0.601	0.200	958.8	965.4	
	0.334	0.332	0.334	1182.4	1150.5	
	0.597	0.203	0.200	954.6	960.7	
	0.751	0.149	0.100	1026.9	1023.3	

It can be seen in Figure 12 that the deviation from the calculated model data with the experimental data never exceeded ±8%, and that 80% of the experimental data fell within ±3% of the theoretical values.

When the results for the polynomial and the quadruplet model are compared, it is obvious that the differences between the models are random and very small. The similarity of the two models can be explained by the nature of the LiF−NaF−LaF_3 melt. In contrast to, for example, a LiF−BeF_2 melt, in which BeF_2 acts as a chain former, the liquid in this study has a more ionic character. Unfortunately, we do not have spectroscopic data on molten LiF−NaF−LaF_3. This would enable us to determine its structural characteristics, and to therefore select the most appropriate thermodynamic model to describe it; it is an item that should be included in a future study on this system. However, Raman studies on molten LaF_3−KF showed that at mole fractions $X_{LaF_3} \leq 0.25$, the La^{3+} ions are relatively shielded by the F^- ions.[25] At compositions $X_{LaF_3} > 0.25$, the proposed structure of the melt is a loose network of distorted LaF_6^{3-} octahedra bound by shared F^- ions.[26] This implies a weak tendency on this melt to form ternary complexes or chains. For melts with a stronger ordering, it is expected that the quasichemical model with the quadruplet approach should give the better description.

4.3. From Binary to Ternary Systems. The Kohler−Toop method of extrapolating excess Gibbs energy parameters from the binary subsystems to the ternary systems was applied, for the polynomial as well as for the quasichemical approach. This way of extrapolating takes different weights for the components into account, according to their chemical structure and behavior compared to the other components of the system. The method is thus suitable for chemically asymmetric systems, for which the systems studied here are an excellent example, with two univalent and one trivalent fluoride. However, in both models, a comparison has been made by assigning LiF, NaF, and LaF_3 to the same symmetry group, which equalizes the weights. It has been found that the difference in the presented diagrams in Figures 8 and 9 is minimal, up to 10 K. It is more important that the binary diagrams give a satisfactory description, as that influences the shape of the ternary diagram much more than the way of extrapolating Gibbs energies.

To improve the fit with the measured and the calculated ternary eutectics in LiF−NaF−LaF_3 and LiF−NaF−CeF_3, we included ternary interaction terms in the polynomial model as well. However, it appeared that the agreement with the experimental data did not improve.

4.4. Implications for MSR Fuel. The eutectic melt in LiF−NaF−PuF_3 is calculated at 906 K, with a composition of 53.7% LiF, 40.5% NaF, and 5.8% PuF_3. Seen in the light of the Generation IV Molten Salt Reactor, this result implies that a eutectic mixture of LiF−NaF−PuF_3 is suitable as reactor fuel. Nowadays, several projects on the MSR as an actinide burner are underway. The TIER project[27] proposes a fuel composition of NaF, ZrF_4, and up to 3.5% actinide fluoride at an average operating temperature of 923 K. This temperature is also suggested in the Czech SPHINX project,[28] with compositions of LiF−NaF−BeF_2 as the solvent. However, the difference of only 17 K between the calculated melting temperature of the LiF−NaF−PuF_3-based fuel mixture and the designed operating temperature is probably too small, especially when computational uncertainties and the influence of other parameters related to the reactor design are taken into account. For safety reasons, it might be preferable to increase this margin between calculated and operating fuel temperature. This can be achieved by the addition of a melting-point-decreasing compound such as

(25) Dracopolous, V.; Gilbert, B.; Papatheodorou, G. N. *J. Chem. Soc., Faraday Trans.* **1998**, *94*, 2601.

(26) Dracopolous, V.; Gilbert, B.; Børrensen, B.; Photiadis, G. M.; Papatheodorou, G. N. *J. Chem. Soc., Faraday Trans.* **1997**, *93*, 3081.

(27) Bowman, R. C. *Once-Through Thermal-Spectrum Accelerator-Driven System for LWR Waste Destruction Without Reprocessing: Tier-1 Description*; Report ADNA 98-04; ADNA Corp.: Los Alamos, NM, August 1998.

(28) Hron, M.; Mikisek, M. In *Atelier GEDEON−PRACTIS*; Les Réacteurs à Sels Fondus et la Pyrochimie: Cadarache, France, 2002; cd-rom.

(29) Holm, J. L.; Kleppa, O. J. *Inorg. Chem.* **1969**, *8*, 207.

(30) Van der Meer, J. P. M.; Konings, R. J. M.; Jacobs, M. H. G.; Oonk, H. A. J. *J. Nucl. Mater.* **2004**, *335*, 345.

(31) Konings, R. J. M.; Van der Meer, J. P. M.; Walle, E. *Chemical Aspects of Molten Salt Reactor Fuel*, Technical Report JRC-ITU-TN 2005/25; European Commission, Joint Research Centre: Brussels, Belgium, 2005.

BeF_2 and/or ZrF_4, which we will address in the next phase of our work.

5. Conclusions

Thermodynamic assessments using our own DSC data have been performed on the binary subsystems of LiF−NaF−LaF_3 and LiF−NaF−CeF_3. Two models were used to describe the excess Gibbs energy parameters of the LiF−NaF−LaF_3 system: a general polynomial and the quasichemical model in the quadruplet approximation. The values obtained for the excess Gibbs energy parameters were extrapolated into the ternary systems according to the asymmetric Kohler−Toop model, where the trifluoride was selected as the asymmetrical component. Calorimetric experiments on the ternaries were done as well, and showed that the agreement between calculated and experimental data was good, usually within ±3% of the measured value. It also appeared that the difference between the two models is minor, which is probably due to the simple ionic nature of the melt. To describe the ternary system of LiF−NaF−PuF_3, which has not yet been measured, we applied a similar method of extrapolating the optimized binary excess Gibbs energy parameters by the polynomial model. The eutectic melt appeared to be at 906 K and a composition of 53.7% LiF, 40.5% NaF, and 5.8% PuF_3, which makes it suitable for Molten Salt Reactor fuel, as proposed in the Generation IV initiative. However, for safety reasons, the liquidus temperature of a LiF−NaF−PuF_3-based fuel mixture might have to be lowered by the addition of BeF_2 and/or ZrF_4. Future work will include the thermodynamic modeling of these multicomponent systems.

Acknowledgment. We thank Herwin Hein for his technical assistance.

CM051531V